SAGA-HE-117-97 (hep-ph/9707220) October 28, 1997

Numerical solution of Q^2 evolution equations for polarized structure functions

M. Hirai, S. Kumano, and M. Miyama *

Department of Physics, Saga University, Saga 840, Japan

ABSTRACT

We investigate numerical solution of Dokshitzer-Gribov-Lipatov-Altarelli-Parisi (DGLAP) Q^2 evolution equations for longitudinally polarized structure functions. Flavor nonsinglet and singlet equations with next-to-leading-order α_s corrections are studied. A brute-force method is employed. Dividing the variables x and Q^2 into small steps, we simply solve the integrodifferential equations. Numerical results indicate that accuracy is better than 1% in the region $10^{-5} < x < 0.8$ if more than two-hundred Q^2 steps and more than one-thousand x steps are taken. Our evolution results are compared with polarized experimental data of the spin asymmetry A_1 by the SLAC-E130, SLAC-E143, EMC, and SMC collaborations. The comparison indicates that we cannot assume A_1 is independent of Q^2. We provide a FORTRAN program for the Q^2 evolution and devolution of polarized nonsinglet-quark, singlet-quark, $\Delta q_i + \Delta\bar{q}_i$, and gluon distributions (and corresponding structure functions).

---

* Email: 96sm18@edu.cc.saga-u.ac.jp, kumanos@cc.saga-u.ac.jp, and 96td25@edu.cc.saga-u.ac.jp. Information on their research is available at http://www.cc.saga-u.ac.jp/saga-u/riko/physics/quantum1/structure.html.

published as Comput. Phys. Commun. 108 (1998) 38.

Program Summary

Title of program: BFP1

Computer: AlphaServer 2100 4/200; *Installation:* The Research Center for Nuclear Physics in Osaka

Operating system: OpenVMS V6.1

Programming language used: FORTRAN 77

Peripherals used: Laser printer

No. of lines in distributed program, including test data, etc.: 1617

Keywords: Structure function, polarized parton distribution, Q^2 evolution, numerical solution.

Nature of physical problem
This program solves DGLAP Q^2 evolution equations with or without next-to-leading-order α_s effects for longitudinally polarized parton distributions. The evolved distributions could be convoluted with coefficient functions for calculating the structure function g_1. Both flavor-nonsinglet and singlet cases are provided, so that the distributions, $x\Delta q_{_{NS}}$, $x\Delta q_{_S}$, $x\Delta q_i^+ \equiv x\Delta q_i + x\Delta \bar{q}_i$ (i=quark flavor), $x\Delta g$, $xg_{1_{NS}}$, xg_{1_S}, and $xg_{1,i}^+$ can be obtained.

Method of solution
The DGLAP integrodifferential equations are simply solved by a brute-force method. We divide the variables x and Q^2 into very small steps, and the integrodifferential equations are solved step by step.

Restrictions of the program
This program is used for calculating Q^2 evolution of a longitudinally polarized flavor-nonsinglet-quark, singlet-quark, Δq_i^+, and gluon distributions in the leading order or in the next-to-leading order of α_s. Q^2 evolution equations are the DGLAP equations. The double precision arithmetic is used. The renormalization scheme is the modified minimal subtraction scheme ($\overline{MS}$). A user provides the initial distribution as a subroutine or as a data file. Examples are explained in section 4. Then, the user inputs fifteen parameters in section 4.

Typical running time
Approximately seven minutes on AlphaServer 2100 4/200 in the nonsinglet case, sixty minutes in the singlet-quark evolution.

LONG WRITE-UP

1 Introduction

Spin structure of the proton has been investigated by polarized lepton-proton scattering. In particular, the structure function g_1 provides us information on the probability to find a quark polarized along the direction of longitudinally polarized proton spin minus the one polarized oppositely. Experimentally, it is measured by a spin asymmetry in the lepton-proton scattering. The g_1 is a function of two kinematical variables Q^2 and $x = Q^2/(2p \cdot q)$, where p is the proton momentum and Q^2 is given by the four-momentum transfer q as $Q^2 = -q^2$. The x dependence is associated with nonperturbative physics, so that x distributions of polarized parton distributions are obtained by fitting various experimental data. At this stage, the only way to study the parton x distributions theoretically is to use phenomenological quark models. On the other hand, the Q^2 dependence is well predicted in perturbative QCD. In general, structure functions are almost independent of the scale Q^2, which is called Bjorken scaling. However, even though it is small, scaling-violation phenomena are observed. The experimental data support perturbative QCD predictions.

As a way of describing the scaling violation, Dokshitzer-Gribov-Lipatov-Altarelli-Parisi (DGLAP) equations [1] are usually used. They are coupled integrodifferential equations. Because the DGLAP equations are frequently used in theoretical and experimental studies, it is worth while creating a program to solve them accurately. We have been studying this topic last several years in a Laguerre-polynomial method [2] and in a brute-force method [3, 4]. Here, we extend the studies to the spin-dependent case. Fortunately, the next-to-leading-order (NLO) splitting functions are calculated recently for polarized parton distributions [5]. It enables us to investigate the details of NLO effects on the Q^2 evolution. We create a FORTRAN program for obtaining numerical solution of the polarized DGLAP equations with the NLO effects. With our program, Q^2 evolution of nonsinglet quark, singlet quark, and gluon distributions can be obtained. Furthermore, NLO coefficient functions could be convoluted with the evolved distributions in our program for calculating the g_1 structure function. It is very useful for investigating polarized parton distributions. In fact, our program in a slightly modified form is used for investigating optimum polarized parton distributions by fitting experimental data [6].

We explain the details of our studies in the following. In section 2, the polarized DGLAP Q^2 evolution equations are explained. Then, our numerical solution method is described in section 3. Input parameters and input distributions are discussed in section 4, and essential subroutines in the program are explained in section 5. Numerical results and their comparison with experimental data are discussed in section 6. Summary is given in section 7. Explicit forms of splitting functions and the coefficient functions are listed in Appendices.

2 Q^2 evolution equations

We use the DGLAP equations [1] for studying the Q^2 evolution. Both the leading order (LO) and the next-to-leading order (NLO) cases can be handled by the DGLAP equations. NLO effects are included in the running coupling constant $\alpha_s(Q^2)$ and in the splitting functions $\Delta P_{ij}(x)$. Here, the evolution of polarized parton distributions $\Delta q = q_\uparrow - q_\downarrow$ and $\Delta g = g_{+1} - g_{-1}$ is investigated.

First, the nonsinglet DGLAP equation is given by

$$\frac{\partial}{\partial \ln Q^2}\,\Delta q_{_{NS}}(x,Q^2) \;=\; \frac{\alpha_s(Q^2)}{2\pi}\;\Delta P_{q^\pm,NS}(x) \otimes \Delta q_{_{NS}}(x,Q^2)\ , \tag{2.1}$$

where $\Delta q_{_{NS}}(x,Q^2)$ is a polarized nonsinglet parton distribution, $\Delta P_{q^\pm,NS}$ is the polarized nonsinglet splitting function, and the convolution $\otimes$ is defined by

$$f(x)\otimes g(x) = \int_x^1 \frac{dy}{y} f\left(\frac{x}{y}\right) g(y)\ . \tag{2.2}$$

The notation $q^\pm$ in the splitting function indicates a $\Delta q^+ = \Delta q + \Delta\bar{q}$ or $\Delta q^- = \Delta q - \Delta\bar{q}$ distribution type, which is explained in Appendix A. Instead of Q^2, it is more convenient to use the variable t defined by

$$t \equiv -\frac{2}{\beta_0}\ln\left[\frac{\alpha_s(Q^2)}{\alpha_s(Q_0^2)}\right]\ , \tag{2.3}$$

where β_0 is defined in Appendix A. The parton distribution and the splitting function multiplied by x

$$\widetilde{f}(x) = x f(x) \tag{2.4}$$

satisfy the same integrodifferential equation. Therefore, we rewrite the evolution equation as

$$\frac{\partial}{\partial t}\,\Delta\widetilde{q}_{_{NS}}(x,t) = \Delta\widetilde{P}_{q^\pm,NS}(x)\otimes\Delta\widetilde{q}_{_{NS}}(x,t)\ . \tag{2.5}$$

Next, the singlet evolution is more complicated than the nonsinglet one due to gluon participation in the evolution. The singlet quark distribution is defined by $\Delta\widetilde{q}_s(x,t) \equiv \sum_i^{N_f} x\,\Delta q_i^+$ where i is the flavor, and $\Delta\widetilde{g}(x,t)$ is the gluon distribution. The singlet case is given by

$$\frac{\partial}{\partial t}\begin{pmatrix}\Delta\widetilde{q}_s(x,t)\\ \Delta\widetilde{g}(x,t)\end{pmatrix} \;=\; \begin{pmatrix}\Delta\widetilde{P}_{qq}(x,t) & \Delta\widetilde{P}_{qg}(x,t)\\ \Delta\widetilde{P}_{gq}(x,t) & \Delta\widetilde{P}_{gg}(x,t)\end{pmatrix}\otimes\begin{pmatrix}\Delta\widetilde{q}_s(x,t)\\ \Delta\widetilde{g}(x,t)\end{pmatrix}\ . \tag{2.6}$$

If each flavor evolution is necessary, another equation has to be used in addition to Eq. (2.6). Using the properties of the splitting functions, $\Delta\widetilde{P}^{(1)}_{q_i^+ q_j^+} = \delta_{ij}\,\Delta\widetilde{P}^{(1)}_{q^+,NS} + 2C_F T_R \widetilde{F}_{qq}$ and $\Delta\widetilde{P}^{(1)}_{q_j^+ g} = \Delta\widetilde{P}^{(1)}_{q^+ g}$ (independent of j), we have the evolution equation

$$\begin{aligned}\frac{\partial}{\partial t}\Delta\widetilde{q}_i^{\,+}(x,t) = \Delta\widetilde{P}_{q^+,\,NS}(x)\otimes\Delta\widetilde{q}_i^{\,+}(x,t) + \ 2\,C_F\,T_R\,\widetilde{F}_{qq}(x)\otimes\Delta\widetilde{q}_S(x,t) \\ + \Delta\widetilde{P}_{q_i^+ g}(x)\otimes\Delta\widetilde{g}(x,t)\ . \end{aligned} \tag{2.7}$$

In this case, three coupled integrodifferential equations in Eqs. (2.6) and (2.7) should be solved simultaneously. All the necessary splitting functions $\Delta\tilde{P}$ and $\tilde{F}$ are listed in Appendix A.

We discuss the NLO effects in the evolution equations. The NLO contributions are included in the running coupling constant $\alpha_s(t)$, in the splitting functions $\Delta P_{ij}(z)$, and in the coefficient functions. Once the NLO corrections are included in the evolution, the renormalization scheme has to be specified. We use the $\overline{MS}$ scheme throughout this paper.

The running coupling constant in the leading order (LO) is given by

$$\alpha_s^{LO}(Q^2) = \frac{4\pi}{\beta_0\ln(Q^2/\Lambda^2)}\ , \tag{2.8}$$

and the one in the next-to-leading order (NLO) is

$$\alpha_s^{NLO}(Q^2) = \frac{4\pi}{\beta_0\ln(Q^2/\Lambda^2)}\left[1-\frac{\beta_1\ln\{\ln(Q^2/\Lambda^2)\}}{\beta_0^2\ln(Q^2/\Lambda^2)}\right]\ . \tag{2.9}$$

The constants β_0 and β_1 are defined in Appendix A. The splitting functions have the perturbative-expansion form

$$\Delta P_{ij}(x) = \Delta P_{ij}^{(0)}(x) + \frac{\alpha_s(Q^2)}{2\pi}\,\Delta P_{ij}^{(1)}(x)\ . \tag{2.10}$$

The second term is the NLO contributions to the splitting functions. The functions are expressed by the ones multiplied by x ($\Delta\widetilde{P}$). Changing the variable Q^2 to t in the DGLAP equations, we have the splitting functions

$$\Delta\widetilde{P}_{ij}(x) = \Delta\widetilde{P}_{ij}^{(0)}(x) + \frac{\alpha_s(t)}{2\pi}\Delta R_{ij}(x)\ , \tag{2.11}$$

where the function $\Delta R_{ij}(x)$ is

$$\Delta R_{ij}(x) \equiv \Delta\widetilde{P}_{ij}^{(1)}(x) - \frac{\beta_1}{2\beta_0}\,\Delta\widetilde{P}_{ij}^{(0)}(x)\ . \tag{2.12}$$

The second term in Eq. (2.12) appears because of the transformation from Q^2 to t. To be precise, the splitting functions $\Delta\widetilde{P}_{ij}$ in Eq. (2.11) should be denoted, for example,

$\Delta\widetilde{P}'_{ij}$ because it is different from $x\Delta P_{ij} = x\Delta P_{ij}^{(0)} + (\alpha_s/2\pi)x\Delta P_{ij}^{(1)}$ which is Eq. (2.10) multiplied by x. (Note the definition of $\tilde{f}$ is $\tilde{f} = xf$.) However, we use the expression without the prime throughout this paper for simplicity. We have the same expression $\Delta\widetilde{P}_{NS} = \Delta\widetilde{P}_{NS}^{(0)} + \alpha_s/(2\pi)\Delta R_{NS}$ in the nonsinglet case.

Next, we discuss the spin-dependent structure function g_1. We have discussed how the Q^2 evolution of quark and gluon distributions is described. However, these parton distributions are not observed directly in experiments. The g_1 could be measured in the polarized lepton-proton scattering with information on the unpolarized structure function F_1. In the LO case, it is given in parton model as

$$xg_1(x) = \frac{1}{2}\sum_i^{N_f} e_i^2 \, \Delta\widetilde{q}_i^{\,+}(x) \ . \tag{2.13}$$

The NLO effects in the structure function are included in the coefficient functions and also in the quark and gluon distributions. In the NLO case, the quark distributions should be convoluted with a coefficient function. Furthermore, an additional gluon correction term should be taken into account:

$$xg_1(x) = \frac{1}{2}\sum_i^{N_f} e_i^2 \, \left[\Delta\widetilde{C}_q(x) \otimes \Delta\widetilde{q}_i^{\,+}(x) + \Delta\widetilde{C}_g(x) \otimes \Delta\widetilde{g}(x) \right] \ , \tag{2.14}$$

where $\Delta\widetilde{C}_q/x$ and $\Delta\widetilde{C}_g/x$ are the quark and gluon coefficient functions in Appendix B. The calculation procedure for the g_1 evolution is the following. First, the Q^2 evolution of the quark and gluon distributions is calculated. Then, the structure function g_1 at Q^2 is evaluated by using Eq. (2.13) or (2.14). An example is explained in section 6.2.

3 Brute-force method

Among various methods of solving the DGLAP equations, we decide to employ a brute-force method. So far, we have investigated two methods, the Laguerre-polynomial [2] and the brute-force [3] methods, in the spin-independent case. The Laguerre method has an advantage of computing time. However, numerical accuracy becomes slightly worse in the nonsinglet case at small x. As far as we studied, the situation is better in the polarized distributions. However, we find a tendency that the accuracy is slightly worse at small x. In light of future HERA spin physics, our program should be accurately enough even at $x = 10^{-5}$. Therefore, we consider that the brute-force method is safer for getting accurate results in the wide x range. The variables x and t are divided into small steps, then integration and differentiation are defined by

$$\frac{df(x)}{dx} = \frac{f(x_{m+1}) - f(x_m)}{\delta x_m} \ , \tag{3.1}$$

$$\int f(x)\ dx = \sum_{m=1}^{N_x} \delta x_m f(x_m) \ . \tag{3.2}$$

With these replacements, the evolution equations could be solved rather easily. For example, Eq. (2.5) is written in the following form:

$$\Delta\widetilde{q}_{NS}(x_k, t_{j+1}) = \Delta\widetilde{q}_{NS}(x_k, t_j) + \delta t_j \sum_{m=k}^{N_x} \frac{\delta x_m}{x_m}\, \Delta\widetilde{P}_{q^\pm,NS}\left(\frac{x_k}{x_m}\right)\, \Delta\widetilde{q}_{NS}(x_m, t_j) \ . \tag{3.3}$$

First, the evolution from $t_0 = 0$ to $t_1 = \delta t$ is calculated in the above equation by providing the initial distribution $\Delta\widetilde{q}_{NS}(x_m, t_{j=1})$. Repeating this step $N_t - 1$ times, we obtain the final distribution at t_{N_t}. Accurate results cannot be obtained at small x if the linear x step is taken ($\delta x = 1/N_x$). Therefore, the logarithmic-x step $\delta(log_{10}x) = |log_{10}x_{min}|/N_x$ is taken in our evolution calculations.

The same method can be applied to the singlet and Δq_i^+ evolution equations in Eqs. (2.6) and (2.7). These equations are written in the brute-force method as:

$$\begin{aligned} \Delta\widetilde{q}_i{}^+(x_k, t_{j+1}) =& \Delta\widetilde{q}_i{}^+(x_k, t_j) \ + \ \delta t_j \sum_{m=k}^{N_x} \frac{\delta x_m}{x_m}\, \Delta\widetilde{P}_{q^+,NS}\left(\frac{x_k}{x_m}\right)\, \Delta\widetilde{q}_i^+(x_m, t_j) \\ &+ \ \delta t_j \sum_{m=k}^{N_x} \frac{\delta x_m}{x_m}\, 2\, C_F\, T_R\, \widetilde{F}_{qq}\left(\frac{x_k}{x_m}\right)\, \Delta\widetilde{q}_S(x_m, t_j) \\ &+ \ \delta t_j \sum_{m=k}^{N_x} \frac{\delta x_m}{x_m}\, \Delta\widetilde{P}_{q_i^+ g}\left(\frac{x_k}{x_m}\right)\, \Delta\widetilde{g}(x_m, t_j) \ , \end{aligned} \tag{3.4a}$$

$$\Delta\widetilde{q}_{S}(x_k,t_{j+1}) = \Delta\widetilde{q}_{S}(x_k,t_j) \ + \ \delta t_j \sum_{m=k}^{N_x} \frac{\delta x_m}{x_m} \, \Delta\widetilde{P}_{qq}\left(\frac{x_k}{x_m}\right) \ \Delta\widetilde{q}_{S}(x_m,t_j)$$

$$+ \ \delta t_j \sum_{m=k}^{N_x} \frac{\delta x_m}{x_m} \, \Delta\widetilde{P}_{qg}\left(\frac{x_k}{x_m}\right) \ \Delta\widetilde{g}(x_m,t_j) \ , \tag{3.4b}$$

$$\Delta\widetilde{g}(x_k,t_{j+1}) = \Delta\widetilde{g}(x_k,t_j) \ + \ \delta t_j \sum_{m=k}^{N_x} \frac{\delta x_m}{x_m} \, \Delta\widetilde{P}_{gq}\left(\frac{x_k}{x_m}\right) \ \Delta\widetilde{q}_{S}(x_m,t_j)$$

$$+ \ \delta t_j \sum_{m=k}^{N_x} \frac{\delta x_m}{x_m} \, \Delta\widetilde{P}_{gg}\left(\frac{x_k}{x_m}\right) \ \Delta\widetilde{g}(x_m,t_j) \ . \tag{3.4c}$$

These are coupled equations. However, they can be solved by providing the initial distributions, $\Delta\widetilde{q}_i^{\,+}(x_m,t_{j=0})$, $\Delta\widetilde{q}_{S}(x_m,t_{j=0})$, and $\Delta\widetilde{g}(x_m,t_{j=0})$, and by repeating the evolution step N_t times.

We should be careful in handling $1/(1-x)_+$ terms in the splitting functions. They are given in our method by

$$\int_x^1 dx' \frac{f(x')}{(1-x')_+} = \sum_{m=k}^{N_x} \delta x_m \, \frac{f(x_m)-f(1)}{1-x_m} \ + \ f(1) \, \ln(1-x_k) \ . \tag{3.5}$$

In the same way, the integral with $[\ln(1-x)/(1-x)]_+$ becomes

$$\int_x^1 dx' f(x') \left[\frac{\ln(1-x')}{1-x'}\right]_+ = \sum_{m=k}^{N_x} \delta x_m \, [f(x_m)-f(1)] \, \frac{\ln(1-x_m)}{1-x_m}$$

$$+ \frac{1}{2} \, f(1) \, \ln^2(1-x_k) \ . \tag{3.6}$$

4 Description of input parameters and input distribution

For running the FORTRAN-77 program BFP1, a user should supply fifteen input parameters from the file #10. In addition, an input distribution(s) should be given in a function subroutine(s) in the end of the FORTRAN program or in an input data file(s), #13, #14, and/or #15. The initial distribution(s) could be written in the output file #12. Evolution results are written in the output file #11. We explain the input parameters and the input distributions in the following.

4.1 Input parameters

There are fifteen parameters. Numerical values of the parameters should be supplied in the file #10, then these are read in the main program.

IOUT	1	write x and $x\Delta q_{NS}(x)$ [or $xg_{1_{NS}}(x)$] at fixed Q^2 (=Q2) in the file #11
	2	write Q^2 and $x\Delta q_{NS}(Q^2)$ [or $xg_{1_{NS}}(Q^2)$] at fixed x (=XX) in the file #11
	3	x, $x\Delta q_S(x)$ [or $xg_{1_S}(x)$], and $x\Delta g(x)$
	4	Q^2, $x\Delta q_S(Q^2)$ [or $xg_{1_S}(Q^2)$], and $x\Delta g(Q^2)$
	5	x, $x\Delta q_i^+(x)$ [or $xg_{1,i}^+(x)$], $x\Delta q_S(x)$ [or $xg_{1_S}(x)$], and $x\Delta g(x)$ [or $xg_{1,g}(x)$]
	6	Q^2, $x\Delta q_i^+(Q^2)$ [or $xg_{1,i}^+(Q^2)$], $x\Delta q_S(Q^2)$ [or $xg_{1_S}(Q^2)$], and $x\Delta g(Q^2)$ [or $xg_{1,g}(x)$]
IREAD	1	give initial distribution(s) in function subroutine(s)
	2	read initial distribution(s) from data file(s)
INDIST	1	do not write initial distribution(s)
	2	write initial distribution(s) in the file #12
	3	write initial distribution(s) in the file #12 without calculating evolution
IORDER	1	leading order (LO) in α_s
	2	next-to-leading order (NLO)
ITYPE	1	structure function $xg_1(x, Q^2)$
	2	quark distribution $x\Delta q(x, Q^2)$ and gluon distribution $x\Delta g(x, Q^2)$
IMORP	1	$x\Delta q_i - x\Delta\bar{q}_i$ type distribution
	2	$x\Delta q_i + x\Delta\bar{q}_i$ type distribution

Q02	initial Q^2 ($\equiv Q_0^2$ in GeV^2) at which an initial distribution is supplied
Q2	Q^2 to which the distribution is evolved ($Q^2 \neq Q_0^2$, $Q^2 > Q_0^2$ or $Q^2 < Q_0^2$)
DLAM	QCD scale parameter Λ_{QCD} in GeV
NF	number of quark flavors
XX	x at which Q^2 dependent distributions are written (IOUT=2, 4, or 6 case)
NX	number of x steps (NX<5000)
NT	number of t steps (NT<5000)
NSTEP	number of x steps or t steps for writing output distribution(s)
NXMIN	log_{10}(minimum of x) [$0 < min(x) = 10^{NXMIN} < XX$]

The meaning of IREAD is explained in section 4.2. The structure function xg_1^p is obtained by the convolution of the distributions, $(1/2)[(4/9)x(\Delta u + \Delta\bar{u} + \Delta c + \Delta\bar{c}) + (1/9)x(\Delta d + \Delta\bar{d} + \Delta s + \Delta\bar{s})]$ and $x\Delta g$ in the four flavor case, with the corresponding coefficient functions. Practically, we use the expression $(1/2)\sum_i e_i^2 x\Delta q_i = (1/2)x[4\Delta q_s - 3(\Delta d^+ + \Delta s^+)]/9$, where $\Delta d^+ = \Delta d + \Delta\overline{d}$ and $\Delta s^+ = \Delta s + \Delta\overline{s}$, instead of the above one in calculating xg_1. It is explained in more detail in section 6.2. The expression could be used only in the four and three flavor cases. In the five or six flavor evolution, it should be slightly modified. The parameter IMORP indicates a plus or minus type distribution $\sum_i a_i x(\Delta q_i \pm \Delta\bar{q}_i)$, where a_i are some constants. IMORP=1 or 2 should be taken in the nonsinglet evolution. In the singlet or Δq_i^+ case, IMORP=2 should be chosen.

For example, if one would like to evolve an initial singlet-quark distribution $x\Delta q_{_S}$ at Q^2=4 GeV^2 to the distribution at Q^2=200 GeV^2 by the NLO DGLAP equations with N_f=4 and Λ=0.231 GeV, the input parameters could be IOUT=3, IREAD=1, INDIST=1, IORDER=2, ITYPE=2, IMORP=2, Q02=4.0, Q2=200.0, DLAM=0.231, NF=4, XX=0.0, NX=1000, NT=200, NSTEP=100, and NXMIN=−4. In this case, the input file #10 is the following:

```
3, 1, 1, 2, 2, 2
4.0, 200.0, 0.231, 4, 0.0, 1000, 200, 100, −4  .
```

4.2 Input distributions supplied by function subroutines (IREAD=1)

If IREAD=1 is chosen, an input distribution(s) at Q_0^2 should be supplied in the end of the FORTRAN program BFP1 as a function subroutine(s).

1) Nonsinglet case

An initial nonsinglet-quark distribution at Q_0^2 should be given in QNS0(X) as a double precision function. As an example, the GS (set A) valence quark distribution $x\Delta u_v + x\Delta d_v$ [7] at Q_0^2=4 GeV^2 is given in the program BFP1.

2) Singlet case

An initial singlet-quark distribution at Q_0^2 should be supplied in QS0(X), and an initial gluon distribution in the nucleon should be in G0(X). The GS $x\Delta q_{_S} = x\Delta u_v + x\Delta d_v + 6x\Delta S$ and $x\Delta g$ distributions are given in the program.

3) Δq_i^+ distribution case

In addition to the above $x\Delta q_{_S}$ and $x\Delta g$ distributions, the initial $x\Delta q_i^+$ distribution (and another flavor distribution $x\Delta q_j^+$) should be supplied. In calculating two-flavor distributions simultaneously for obtaining xg_1, two distributions (e.g. $x\Delta d^+$ and $x\Delta s^+$) should be supplied in the functions QI0(1,x) and QI0(2,x). If one needs only one-flavor evolution, one may set QI0(2,x)=0. The GS distributions $x\Delta d^+$ and $x\Delta s^+$ are given in our program as an example.

4.3 Input distributions supplied by data files (IREAD=2)

If IREAD=2 is chosen, an input distribution(s) at Q_0^2 should be supplied in a separate data file(s).

1) Nonsinglet case (data file #13)

An initial nonsinglet-quark distribution at Q_0^2 should be given in the data file #13 as shown in the following example.

0.000100	0.009761
0.000110	0.010184
0.000120	0.010624
0.000132	0.011081
0.000145	0.011555
...	...
...	...
...	...
1.000000	0.000000

The first column is the x values and the second one is the corresponding $x\Delta u_v + x\Delta d_v$ values. The data at $x \le x_{min}$ and at x=1.0 must be supplied.

2) Singlet case in the nucleon (data file #14)

An initial singlet-quark distribution and a gluon distribution should be given in the data file #14 as shown in the following.

0.000100	0.001721	0.006729
0.000110	0.001612	0.007193
0.000120	0.001485	0.007688
0.000132	0.001339	0.008218
0.000145	0.001172	0.008784
...	...	...
...	...	...
...	...	...
1.000000	0.000000	0.000000

The first column is the x values, the second is the $x\Delta q_S$ distribution, and the third is the $x\Delta g$ distribution. The data at $x \le x_{min}$ and at x=1.0 must be supplied.

3) Δq_i^+ distribution case (data file #15)

An initial Δq_i^+ distribution, a singlet-quark distribution, and a gluon distribution should be given in the data file #15 as shown in the following.

0.000100	-0.003637	-0.002681	0.001721	0.006729
0.000110	-0.003884	-0.002859	0.001612	0.007193
0.000120	-0.004147	-0.003048	0.001485	0.007688
0.000132	-0.004428	-0.003249	0.001339	0.008218
0.000145	-0.004727	-0.003462	0.001172	0.008784
...	...	...	...	...
...	...	...	...	...
...	...	...	...	...
1.000000	0.000000	0.000000	0.000000	0.000000

The first column is the x values, the second is the $x\Delta q_i^+$ distribution, the third is another flavor distribution $x\Delta q_j^+$, the fourth is $x\Delta q_S$, and the fifth is $x\Delta g$. The data at $x \le x_{min}$ and at x=1.0 must be supplied. If one needs only one-flavor evolution, the second or third column values are set to 0.

5 Description of the program BFP1

The major part of the program BFP1 is essentially the same as the unpolarized version [3]. We do not explain each subroutine in this section. They are already well described in the previous publication, so that the interested reader may read Ref. [3] for the detailed description of all the subroutines.

The main program reads fifteen input parameters from the input file #10. Actual Q^2 evolution calculations are done by calling the subroutine GETQNS in the nonsinglet case and GETQS in the singlet (or $x\Delta q_i$) case. Each evolution step is calculated by the subroutine QNSXT or GETQGX. Minor modifications are made in each flavor evolution (GETQS) so that two quark distributions ($x\Delta q_i^+$ and $x\Delta q_j^+$) are evolved simultaneously. A typical function of the GS parton distributions is given as the function GS(X,A,B,C,D,E,F). We explain the subroutines associated with the input distributions in the following.

5.1 Function GS(X,A,B,C,D,E,F)

This function calculates the GS parton distributions given by the parameters A, B, C, D, E, and F as $ABx^C(1-x)^D(1+Ex+F\sqrt{x})$.

5.2 Functions QNS0(X), QS0(X), G0(X), and QI0(I,X)

The functions QNS0, QS0, and G0 calculate an initial nonsinglet-quark distribution $x\Delta q_{NS}$, a singlet-quark distribution $x\Delta q_S$, and a gluon distribution $x\Delta g$. As an example, the GS distributions [7] are provided.
The nonsinglet one is

$$\begin{aligned} QNS0 =& x\Delta u_v + x\Delta d_v \\ =& 0.918 * 1.365x^{0.512}(1-x)^{3.96}(1+11.65x-4.6\sqrt{x}) \\ &+ (-0.339) * 3.849x^{0.78}(1-x)^{4.96}(1+7.81x-3.48\sqrt{x}) \ , \end{aligned} \tag{5.1}$$

the singlet one in the three flavor case is

$$\begin{aligned} QS0 =& x\Delta u_v + x\Delta d_v + 6x\Delta S \\ =& 0.918 * 1.365x^{0.512}(1-x)^{3.96}(1+11.65x-4.6\sqrt{x}) \\ &+ (-0.339) * 3.849x^{0.78}(1-x)^{4.96}(1+7.81x-3.48\sqrt{x}) \\ &+ 6 * (-0.06) * 18.521x^{0.724}(1-x)^{14.4}(1+4.63x-4.96\sqrt{x}) \ , \end{aligned} \tag{5.2}$$

and the gluon distribution is

$$G0 = 1.71 * 3.099x^{0.724}(1-x)^{5.71}(1+0.0x+0.0\sqrt{x}) \ . \tag{5.3}$$

The function QI0 calculates two initial flavor distributions. As an example, the GS $x\Delta d^+ = x\Delta d + x\Delta\overline{d}$ and $x\Delta s^+ = x\Delta s + x\Delta\overline{s}$ distributions are provided:

$$\begin{aligned} QI0_1 =& x\Delta d_v + 2x\Delta\bar{d} \\ =& -0.339 * 3.849x^{0.78}(1-x)^{4.96}(1+7.81x-3.48\sqrt{x}) \\ &+ 2*(-0.06)*18.521x^{0.724}(1-x)^{14.4}(1+4.63x-4.96\sqrt{x}) \ , \end{aligned} \tag{5.4}$$

$$\begin{aligned} QI0_2 =& 2x\Delta s \\ =& 2*(-0.06)*18.521x^{0.724}(1-x)^{14.4}(1+4.63x-4.96\sqrt{x}) \ . \end{aligned} \tag{5.5}$$

In these equations, the flavor symmetry $\Delta\bar{u} = \Delta\bar{d} = \Delta\bar{s} = \Delta S$ is assumed.

6 Numerical analysis

6.1 Accuracy of Q^2 evolution results

There are two parameters which determine the accuracy of our numerical results. They are the numbers of steps: N_x and N_t. As they become larger, the accuracy becomes better. However, there is a restriction because the evolution computation should be done within a certain CPU time depending on the machine power. We check how the evolution results depend on these parameters and how long it takes for finishing the evolution.

First, we fix the x step at N_x=1000, then the t step N_t is varied as 20, 50, 200, and 1000. Numerical results for the polarized singlet quark distribution are shown in Fig. 1. The initial distribution is the GS-A at Q^2=4 GeV^2 [7]. The three-flavor distribution is considered. Because there is little information on each antiquark distribution [9], flavor symmetric distributions are assumed for the antiquark distributions. The scale parameter is taken as Λ=231 MeV in fitting polarized experimental data. We use N_f =4 and Λ=231 MeV for calculating the evolution. The GS-A singlet distribution is evolved to the one at Q^2=200 GeV^2 by our NLO program. The input distribution is supplied in the end of the program as the subroutine QS0. The input parameters are IOUT=3, IREAD=1, INDIST=1, IORDER=2, ITYPE=2, IMORP=2, Q02=4.0, Q2=200.0, DLAM=0.231, NF=4, XX=0.0, NX=1000, NT=200, NSTEP=100, and NXMIN=-4. There is almost no difference between the various results in Fig. 1, which means that merely fifty steps are enough for getting accurate evolution. This is certainly expected from the fact that the scaling violation is a small logarithmic effect.

Next, the step N_x is varied with fixed N_t=200 in Fig. 2. N_x=100, 300, 1000, and 4000 are taken. Even in the 300 steps, we obtain rather accurate results. The evolution results become slightly worse in the gluon case as shown in Figs. 3 and 4. Defining the evolution accuracy by $|\,[\Delta p(N_x,N_t)-\Delta p(N_x=4000,N_t=1000)]/\Delta p(N_x=4000,N_t=1000)\,|$, we find that the accuracy is better than 1% in the region $10^{-5}<x<0.8$ with $N_x=1000$ and $N_t=200$. However, it takes rather a significant amount of running CPU time. It is typically seven minutes on the AlphaServer 2100 4/200 in a nonsinglet case and sixty minutes in a singlet case. Our program is good enough for a single evolution calculation, but it is not efficient enough for repeated use. We will work on a much faster program in future.

We also check our results with other publications. First, the evolution in Ref. [7] from Q^2=4 GeV^2 to Q^2=50 GeV^2 are compared with our results. The structure functions xg_1^p and xg_1^n at Q^2=50 GeV^2 agree well with our evolved ones. Second, the evolution in Ref. [10] is compared with ours. The GS-A input distributions are used. They are evolved to the ones at Q^2=10 GeV^2 with Λ=239 MeV and are also devolved to the ones at Q^2=2 GeV^2. The singlet distribution Δq_s and the gluon distribution Δg are compared. We find that they agree well with our evolution results. From these studies on our results in comparison with others and from repeated checks on our evolution program, we find that the program BFP1 is reliable. We should mention that there is another work [11] on the NLO evolution in addition to Refs. [7] and [10].

6.2 Calculation of g_1 from output data

We do not supply the BFP1 program so that the structure function g_1 is obtained directly in the output file. It is because g_1 depends on the number of flavor and because the precise evolution should be described by setting flavor thresholds. We ask the reader to set up these points by oneself with our program. Actual evolution results for g_1 are shown in the next subsection, where the following prescription is used for calculating g_1 from the output data file #11.

First, IOUT=5 or 6 should be chosen so that the evolution of $\Delta q_i^+(x)$, $\Delta q_j^+(x)$, $\Delta q_{_S}(x)$, and $\Delta g(x)$ is calculated by Eqs. (2.6) and (2.7). Furthermore, ITYPE=1 should be chosen for calculating the convolution integrals of these evolved distributions with the coefficient functions in Eq. (2.14). The convolution results are written in the output file #11, and we denote them as $g_{1,d}^+(x)$, $g_{1,str}^+(x)$, $g_{1_S}^+(x)$, and $g_{1,g}^+(x)$. It goes without saying that the convolution is not necessary in the LO case. The LO g_1 is calculated directly by Eq. (2.13). Next, the g_1 for the proton is, for example, calculated by choosing $\Delta d^+(x)$ and $\Delta s^+(x)$ for the distributions $\Delta q_i^+(x)$ and $\Delta q_j^+(x)$:

$$\begin{aligned} g_1^p(x,Q^2) &= \frac{1}{2} \sum_i^{N_f} e_i^2 \, \left[g_{1,i}(x,Q^2) + g_{1,g}(x,Q^2) \right] \\ &= \frac{1}{18} \left[4\, g_{1_S}^+(x,Q^2) - 3\, \{ g_{1,d}^+(x,Q^2) + g_{1,str}^+(x,Q^2) \} \right] + \frac{1}{2} \sum_i^{N_f} e_i^2\, g_{1,g}(x,Q^2) \ , \end{aligned} \tag{6.1}$$

in the three and four flavor cases. Five and six flavor evolution can be calculated in the similar way with a slightly modified equation.

6.3 Comparisons with experimental data

We calculate evolution of the structure function g_1 and compare its results with experimental data. Using the procedure in the last subsection, we obtain the evolution results for g_1. The LO and NLO results are shown in Fig. 5. The same GS-A polarized parton distributions are used as the input distributions at Q^2=4 GeV^2 in both LO and NLO cases. To be precise, this is not a correct procedure because the GS-A is set up for the NLO $\overline{MS}$ calculation. It should not be used in the LO calculation. Nevertheless, the GS-A distributions are also employed in the LO for finding NLO effects on g_1. Therefore, the differences between the solid and dashed curves at Q^2=4 GeV^2 are purely due to the coefficient functions. Because the coefficient-function contributions are rather large, it is difficult to find the NLO evolution effects from Fig. 5. In order to illustrate the NLO effects from Q^2=4 GeV^2 to Q^2=200 GeV^2, we show the evolution of the distribution $\sum_i e_i^2\, x\, \Delta q_i/2$ in Fig. 6. The same distributions are taken at Q^2=4 GeV^2 in the LO and NLO cases. The figure indicates that the NLO effects are positive in the small and large x regions and they are negative in the intermediate region $x \approx 0.2$.

Our evolution results are compared with spin-asymmetry data in Figs. 7, 8, and 9. The SLAC-E130 [12], SLAC-E143 [13], EMC [14], and SMC [15] data are shown in the figures. We comment how the spin asymmetry is calculated theoretically. The asymmetry is given by the structure functions g_1 and F_1 as

$$A_1 \cong \frac{g_1(x,Q^2)}{F_1(x,Q^2)} = g_1(x,Q^2)\,\frac{2\,x\,(1+R)}{F_2(x,Q^2)}\ . \tag{6.2}$$

The function R is given by $R = (F_2 - 2xF_1)/(2xF_1)$, and it could be taken from Ref. [16]. In fitting experimental data for obtaining the optimum unpolarized parton distributions, the F_2 structure function is used instead of F_1. Therefore, it is better to calculate the asymmetry with F_2 if we would like to compare with the experimental data. The MRS-G unpolarized parton distributions [17] are used for calculating F_2 and the function R in Ref. [16] is used in Eq. (6.2).

In Fig. 7, our evolution curves at x=0.035 are shown with the asymmetry A_1 data. The dashed and solid curves indicate the LO and NLO evolution results respectively. In the large Q^2 region, both results are almost the same; however, they differ significantly at small Q^2 in particular in the region $Q^2 < 2$ GeV^2. The difference is not so large at slightly larger x (=0.08) as shown in Fig. 8. However, the LO values become larger than those of the NLO evolution. In the medium x region (x=0.25), the difference becomes larger again at small Q^2 as shown in in Fig. 9. From these figures, we find that the asymmetry has Q^2 dependence although it is not large. People used to assume that the asymmetry is independent of Q^2 by neglecting the Q^2 evolution difference between g_1 and F_1 in analyzing the experimental data. We find clearly that it is not the case. For a precise analysis, the Q^2 dependence in the asymmetry has to be taken into account. Currently, parametrization studies are in progress [6] by using our program. We expect to obtain NLO fitting results in the near future.

7 Summary

We have investigated numerical solution of the spin-dependent DGLAP equations with or without the NLO corrections. The solution method is so called brute-force method. A FORTRAN program is provided for evolving longitudinally polarized parton distributions including nonsinglet, singlet, each flavor, and gluon distributions. Furthermore, the evolution results could be written in a structure-function form, which is the convolution of the evolved distributions with the coefficient functions. Therefore, the structure function g_1 could be also calculated from our output data. We checked that typical accuracy is better than 1% with reasonable numbers of steps: N_x=1000 and N_t=200. Comparisons with experimental data indicate significant Q^2 dependence and NLO effects in the region $Q^2 \approx 1$ GeV^2. Therefore, the Q^2 independence assumption, which was used to be employed in analyzing A_1 experimental data, is not valid. We have to include the Q^2 evolution differences between F_1 and g_1. Our evolution code is very useful for theoretical and experimental researchers in high-energy spin physics.

Acknowledgments

MH, SK, and MM thank the Research Center for Nuclear Physics in Osaka for making them use computer facilities. They thank participants, in particular those in Ref. [6], of the RHIC-SPIN-J collaboration meetings for discussions on the polarized parton distributions.

Appendix A. Splitting functions

First, the constants β_0, β_1 C_G, C_F, and T_R are given by the number of color (N_c=3) and the number of flavor (N_f) as

$$\beta_0 = \frac{11}{3} C_G - \frac{4}{3} T_R N_f \ , \quad \beta_1 = \frac{34}{3} C_G^2 - \frac{10}{3} C_G N_f - 2 C_F N_f \ , \tag{A.1}$$

$$C_G = N_c \ , \quad C_F = \frac{N_c^2 - 1}{2 N_c} \ , \quad T_R = \frac{1}{2} \ . \tag{A.2}$$

Splitting function in the leading order(LO) are

$$\begin{aligned}
\Delta P_{NS}^{(0)}(x) &= C_F \left[\frac{2}{(1-x)_+} - 1 - x + \frac{3}{2} \delta(1-x) \right] \ , \\
\Delta P_{q_i^+ q_j^+}^{(0)}(x) &= \delta_{ij} \, \Delta P_{NS}^{(0)}(x) \ , \\
\Delta P_{q_i^+ g}^{(0)}(x) &= 2 \, T_R \, (2x - 1) \ , \\
\Delta P_{g q_i^+}^{(0)}(x) &= C_F \, (2 - x) \ , \\
\Delta P_{gg}^{(0)}(x) &= 2 \, C_G \left[\frac{1}{(1-x)_+} - 2x + 1 \right] + \frac{\beta_0}{2} \delta(1-x) \ ,
\end{aligned} \tag{A.3}$$

where the + function is defined by

$$\int_0^1 dx \, \frac{f(x)}{(1-x)_+} \ = \ \int_0^1 dx \, \frac{f(x) - f(1)}{1 - x} \ . \tag{A.4}$$

It should be noted that the above integration is defined in the region $0 \le x \le 1$.

The NLO splitting functions for $\Delta q_i^+(x)$ and $\Delta g(x)$ are given by [5]

$$\begin{aligned}
\Delta P_{q_i^+ q_j^+}^{(1)}(x) &= \delta_{ij} \, \Delta P_{q^+, NS}^{(1)} + 2 \, C_F \, T_R \, F_{qq} \ , \\
\Delta P_{q_i^+ g}^{(1)}(x) &= C_F \, T_R \, F_{qg}^1(x) + C_G \, T_R \, F_{qg}^2(x) \ , \\
\Delta P_{g q_i^+}^{(1)}(x) &= C_F \, T_R \, N_f \, F_{gq}^1(x) + C_F^2 \, F_{gq}^2(x) + C_F \, C_G \, F_{gq}^3(x) \ , \\
\Delta P_{gg}^{(1)}(x) &= -C_G \, T_R \, N_f \, F_{gg}^1(x) - C_F \, T_R \, N_f \, F_{gg}^2(x) + C_G^2 \, F_{gg}^3(x) \ .
\end{aligned} \tag{A.5}$$

The splitting functions in the singlet equations (2.6) are expressed as

$$\begin{aligned}
\Delta P_{qq} \otimes \Delta q_s &= \sum_{i,j} \Delta P_{q_i^+ q_j^+} \otimes \Delta q_j \ , \quad \Delta P_{qg} \otimes \Delta g = \sum_i \Delta P_{q_i^+ g} \otimes \Delta g \ , \\
\Delta P_{gq} \otimes \Delta q_s &= \sum_j \Delta P_{g q_j^+} \otimes \Delta q_j \ .
\end{aligned} \tag{A.6}$$

The splitting function $\Delta P^{(1)}_{q^\pm,NS}$ is given

$$\Delta P^{(1)}_{q^\pm,NS} = P^{(1)}_{q^\mp,NS} \ , \tag{A.7}$$

where $P^{(1)}_{q^\mp,NS}$ are the unpolarized NLO nonsinglet splitting functions. The $\pm$ in these equations indicates "$\Delta q \pm \Delta\bar{q}$ type" distribution $\sum_i a_i(\Delta q_i \pm \Delta\bar{q}_i)$. The function $\Delta P^{(1)}_{q^\pm,NS}$ is given by

$$\begin{aligned}
\Delta P^{(1)}_{q^\pm,NS}(x) =& C_F^2\left\{ P_F(x) \mp P_A(x) + \delta(1-x)\left[\frac{3}{8} - \frac{1}{2}\pi^2 + \zeta(3) - 8\widetilde{S}(\infty)\right]\right\} \\
&+ \frac{1}{2}C_F C_A\left\{ P_G(x) \pm P_A(x) + \delta(1-x)\left[\frac{17}{12} + \frac{11}{9}\pi^2 - \zeta(3) + 8\widetilde{S}(\infty)\right]\right\} \\
&+ C_F T_R N_f\left\{ P_{N_F}(x) - \delta(1-x)\left(\frac{1}{6} + \frac{2}{9}\pi^2\right)\right\} \ ,
\end{aligned} \tag{A.8}$$

where $P_F(x)$, $P_G(x)$, $P_{N_F}(x)$, and $P_A(x)$ are given in Ref. [18]

$$\begin{aligned}
P_F(x) &= -2\frac{1+x^2}{1-x}\ln x \ln(1-x) - \left(\frac{3}{1-x} + 2x\right)\ln x - \frac{1}{2}(1+x)\ln^2 x - 5(1-x) \ , \\
P_G(x) &= \frac{1+x^2}{(1-x)_+}\left[\ln^2 x + \frac{11}{3}\ln x + \frac{67}{9} - \frac{1}{3}\pi^2\right] + 2(1+x)\ln x + \frac{40}{3}(1-x) \ , \\
P_{N_F}(x) &= \frac{2}{3}\left[\frac{1+x^2}{(1-x)_+}\left(-\ln x - \frac{5}{3}\right) - 2(1-x)\right] \ , \\
P_A(x) &= 2\frac{1+x^2}{1+x}\int_{x/(1+x)}^{1/(1+x)} \frac{dz}{z}\ln\frac{1-z}{z} + 2(1+x)\ln x + 4(1-x) \ .
\end{aligned} \tag{A.9}$$

The functions F_{qq}, F_{qg}, F_{gq}, and F_{gg} are defined by

$$F_{qq}(x) = (1-x) - (1-3x)\ln x - (1+x)\ln^2 x \ , \tag{A.10}$$

$$\begin{aligned}
F^1_{qg}(x) =& -22 + 27x - 9\ln x + 8(1-x)\ln(1-x) \\
&+ \delta p_{qg}(x)\left[2\ln^2(1-x) - 4\ln(1-x)\ln x + \ln^2 x - \frac{2}{3}\pi^2\right] \ , \\
F^2_{qg}(x) =& 2(12-11x) - 8(1-x)\ln(1-x) + 2(1+8x)\ln x \\
&- 2\left[\ln^2(1-x) - \frac{\pi^2}{6}\right]\delta p_{qg}(x) - \left[2S_2(x) - 3\ln^2 x\right]\delta p_{qg}(-x) \ ,
\end{aligned} \tag{A.11}$$

$$F^1_{gq}(x) = -\frac{4}{9}(x+4) - \frac{4}{3}\delta p_{gq}(x)\ln(1-x) \ ,$$
$$F^2_{gq}(x) = -\frac{1}{2} - \frac{1}{2}(4-x)\ln x - \delta p_{gq}(-x)\ln(1-x) + \left[-4 - \ln^2(1-x) + \frac{1}{2}\ln^2 x\right]\delta p_{gq}(x) \ ,$$
$$\begin{aligned} F^3_{gq}(x) = &(4-13x)\ln x + \frac{1}{3}(10+x)\ln(1-x) + \frac{1}{9}(41+35x) \\ &+ \frac{1}{2}[-2S_2(x) + 3\ln^2 x]\delta p_{gq}(-x) \\ &+ \left[\ln^2(1-x) - 2\ln(1-x)\ln x - \frac{\pi^2}{6}\right]\delta p_{gq}(x) \ , \end{aligned} \quad \text{(A.12)}$$

$$\begin{aligned} F^1_{gg}(x) = &\,4(1-x) + \frac{4}{3}(1+x)\ln x + \frac{20}{9}\delta p_{gg}(x) + \frac{4}{3}\delta(1-x) \ , \\ F^2_{gg}(x) = &\,10(1-x) + 2(5-x)\ln x + 2(1+x)\ln^2 x + \delta(1-x) \ , \\ F^3_{gg}(x) = &\,\frac{1}{3}(29-67x)\ln x - \frac{19}{2}(1-x) + 4(1+x)\ln^2 x - 2S_2(x)\delta p_{gg}(-x) \\ &+ \left[\frac{67}{9} - 4\ln(1-x)\ln x + \ln^2 x - \frac{\pi^2}{3}\right]\delta p_{gg}(x) + \left[3\zeta(3) + \frac{8}{3}\right]\delta(1-x) \ , \end{aligned} \quad \text{(A.13)}$$

where, δp_{qg} , δp_{gq} , δp_{gg} are defined

$$\begin{aligned} \delta p_{qg}(x) &\equiv 2x - 1 \ , \\ \delta p_{gq}(x) &\equiv 2 - x \ , \\ \delta p_{gg}(x) &\equiv \frac{1}{(1-x)_+} - 2x + 1 \ . \end{aligned} \quad \text{(A.14)}$$

The ζ function is defined by $\zeta(k) = \sum_{n=1}^{\infty} \frac{1}{n^k}$, and $\zeta(3)$ is given by the numerical value ($\zeta(3)$=1.2020569...). The S_2 function is expressed in terms of the Spence function $S(x)$

$$\begin{aligned} S_2(x) &= \int_{x/(1+x)}^{1/(1+x)} \frac{dz}{z}\ln\frac{1-z}{z} \\ &= S\left(\frac{x}{1+x}\right) - S\left(\frac{1}{1+x}\right) - \frac{1}{2}\left[\ln^2\frac{1}{1+x} - \ln^2\frac{x}{1+x}\right] \ , \end{aligned} \quad \text{(A.15)}$$

where $S(x)$ is defined by

$$S(x) \ = \ \int_x^1 dz\,\frac{\ln z}{1-z} \ . \quad \text{(A.16)}$$

It should be noted that another convention is sometimes used, namely $-S(x)$ may be called the Spence function. It is useful to use a series expansion form for numerical calculations

$$S(x) \ = \ -\sum_{k=1}^{\infty}\frac{(1-x)^k}{k^2} \ . \quad \text{(A.17)}$$

Appendix B. Coefficient functions

The coefficient functions ΔC_q and ΔC_q are [5]

$$\Delta C_q(x,\alpha_s) = \delta(1-x) + \frac{\alpha_s}{2\pi}\,\Delta B_q(x)\ , \tag{B.18}$$

$$\Delta C_g(x,\alpha_s) = \frac{\alpha_s}{2\pi}\,\Delta B_g(x)\ , \tag{B.19}$$

where the functions ΔB_q and ΔB_g are

$$\begin{aligned}\Delta B_q(x) = C_F \Bigg[& (1+x^2)\left\{\frac{\ln(1-x)}{1-x}\right\}_+ - \frac{3}{2}\frac{1}{(1-x)_+} - \frac{1+x^2}{1-x}\ln x \\ & + 2 + x - \left(\frac{9}{2}+\frac{\pi^2}{3}\right)\delta(1-x)\Bigg]\ ,\end{aligned} \tag{B.20}$$

$$\Delta B_g(x) = 2\,T_R\left[(2x-1)\left(\ln\frac{1-x}{x} - 1\right) + 2(1-x)\right]\ . \tag{B.21}$$

References

[1] V. N. Gribov and L. N. Lipatov, Sov. J. Nucl. Phys. 15 (1972) 438 and 675; G. Altarelli and G. Parisi, Nucl. Phys. B 126 (1977) 298; Yu. L. Dokshitzer, Sov. Phys. JETP 46 (1977) 641.

[2] S. Kumano and J. T. Londergan, Comput. Phys. Commun. 69 (1992) 373; R. Kobayashi, M. Konuma, and S. Kumano, Comput. Phys. Commun. 86 (1995) 264.

[3] M. Miyama and S. Kumano, Comput. Phys. Commun. 94 (1996) 185.

[4] W.-K. Tung, private communications.

[5] R. Mertig and W. L. van Neerven, Z. Phys. **C70**, 637 (1996); W. Vogelsang, Phys. Rev. **D54**, 2023 (1996).

[6] RHIC-SPIN-J parametrization group: Y. Goto, N. Hayashi, M. Hirai, H. Horikawa, S. Kumano, M. Miyama, T. Morii, N. Saito, T.-A. Shibata, E. Taniguchi, and T. Yamanishi, research in progress.

[7] T. Gehrmann and W. J. Stirling, Phys. Rev. D. 53 (1996) 6100. Other available distributions are found in Ref. [8].

[8] G. A. Ladinsky, hep-ph/9601287; Parton-distribution-function web sites: http://durpdg.dur.ac.uk/HEPDATA/HEPDATA.html, http://www.phys.psu.edu/~cteq.

[9] S. Kumano, preprint-97-97, submitted to Physics Reports.

[10] T. Weigl and W. Melnitchouk, Nucl. Phys. B465 (1990) 267.

[11] J. Blümlein and A. Vogt, pp. 218-221 in Proceedings of the 12th Symposium on High-Energy Spin Physics, edited by C. W. de Jager et al., World Scientific (1997).

[12] G. Baum et al. (SLAC-E130 collaboration), Phys. Rev. Lett. 51 (1983) 1135.

[13] K. Abe et al. (SLAC-E143 collaboration), Phys. Lett. B 364 (1995) 61.

[14] J. Ashman et al. (EMC collaboration), Phys. Lett. B 206 (1988) 364; Nucl. Phys. B 328 (1989) 1.

[15] D. Adams et al. (SMC collaboration), Phys. Lett. B 329 (1994) 399.

[16] L. W. Whitlow, S. Rock, A. Bodek, S. Dasu, and E.M. Riordan, Phys. Lett. B 250 (1990) 193.

[17] A. D. Martin, W. J. Stirling, and R. G. Roberts, Phys. Lett. B 354 (1995) 155.

[18] G. Curci, W. Furmanski, and R. Petronzio, Nucl. Phys. B 175 (1980) 27.

TEST RUN OUTPUT

IOUT= 3 IREAD= 1 INDIST= 1 IORDER= 2 ITYPE= 2 IMORP= 2
Q02= 4.0000 Q2= 200.000 DLAM= 0.2310 NF= 4
XX= 0.0000000 NX=1000 NT= 200 NSTEP= 50 NXMIN= -4

0.000100	-0.019166	0.097380
0.000120	-0.020672	0.105178
0.000145	-0.022276	0.113534
0.000174	-0.023982	0.122478
0.000209	-0.025790	0.132045
0.000251	-0.027703	0.142266
0.000302	-0.029718	0.153174
0.000363	-0.031833	0.164803
0.000437	-0.034043	0.177185
0.000525	-0.036338	0.190351
0.000631	-0.038707	0.204330
0.000759	-0.041130	0.219150
0.000912	-0.043584	0.234833
0.001096	-0.046036	0.251398
0.001318	-0.048444	0.268856
0.001585	-0.050754	0.287209
0.001905	-0.052898	0.306451
0.002291	-0.054790	0.326559
0.002754	-0.056324	0.347493
0.003311	-0.057372	0.369192
0.003981	-0.057777	0.391566
0.004786	-0.057353	0.414496
0.005754	-0.055883	0.437819
0.006918	-0.053115	0.461325
0.008318	-0.048770	0.484750
0.010000	-0.042545	0.507761
0.012023	-0.034126	0.529949
0.014454	-0.023214	0.550821
0.017378	-0.009552	0.569787
0.020893	0.007027	0.586160
0.025119	0.026539	0.599147
0.030200	0.048784	0.607861
0.036308	0.073276	0.611331
0.043652	0.099181	0.608536
0.052481	0.125309	0.598449
0.063096	0.150159	0.580109

0.075858	0.172073	0.552726
0.091201	0.189500	0.515809
0.109648	0.201326	0.469336
0.131826	0.207180	0.413952
0.158489	0.207504	0.351177
0.190546	0.203229	0.283585
0.229087	0.194990	0.214868
0.275423	0.182213	0.149663
0.331131	0.162801	0.092992
0.398107	0.134220	0.049196
0.478630	0.096195	0.020506
0.575440	0.053887	0.005833
0.691831	0.018721	0.000825
0.831764	0.001943	0.000022
1.000000	0.000000	0.000000

Figures

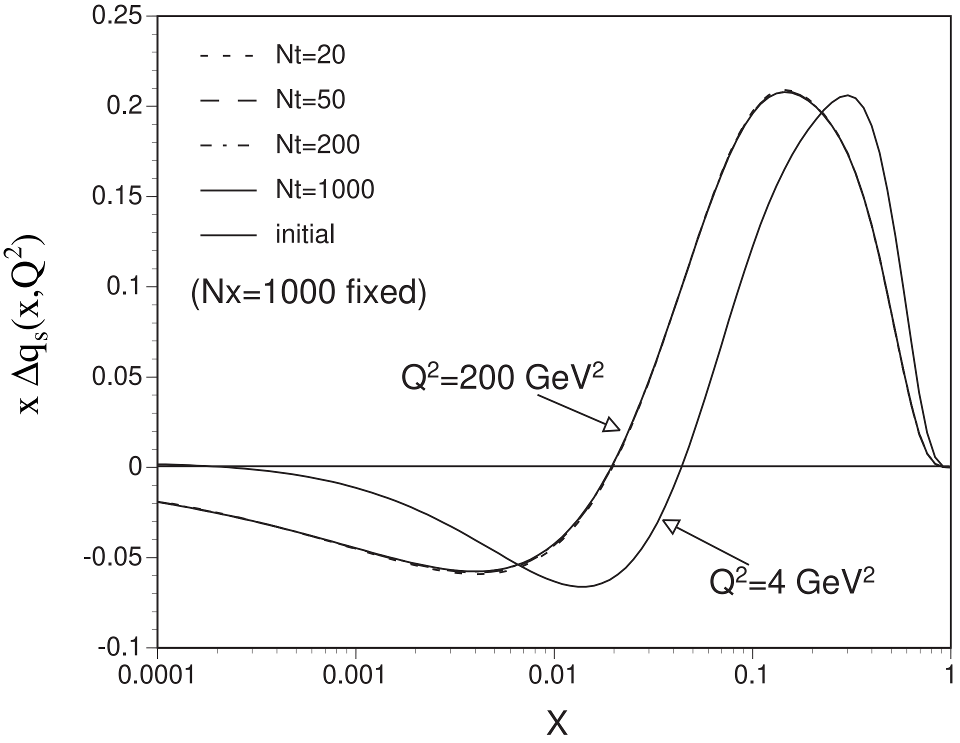

Figure 1: N_t dependence of singlet evolution results is shown. The initial distribution is the GS-A at Q^2=4 GeV^2. It is evolved to the one at Q^2=200 GeV^2 by the next-to-leading-order DGLAP evolution equations. N_x=1000 is fixed and N_t is varied (N_t=20, 50, 200, and 1000). There are dotted, dashed, dot-dashed, and solid curves at Q^2=200 GeV^2 for N_t=20, 50, 200, and 1000 respectively.

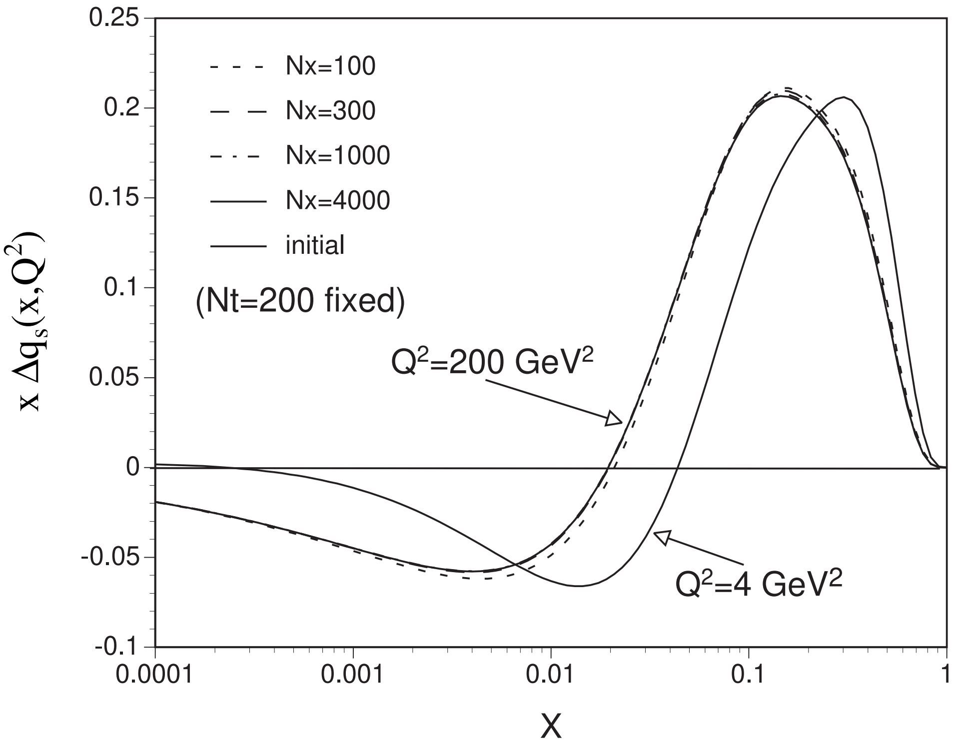

Figure 2: N_x dependence of singlet evolution results is shown. The initial distribution is the same in Fig. 1. N_t=200 is fixed and N_x is varied (N_x=100, 300, 1000, and 4000). There are dotted, dashed, dot-dashed, and solid curves at Q^2=200 GeV^2 for N_x=100, 300, 1000, and 4000 respectively.

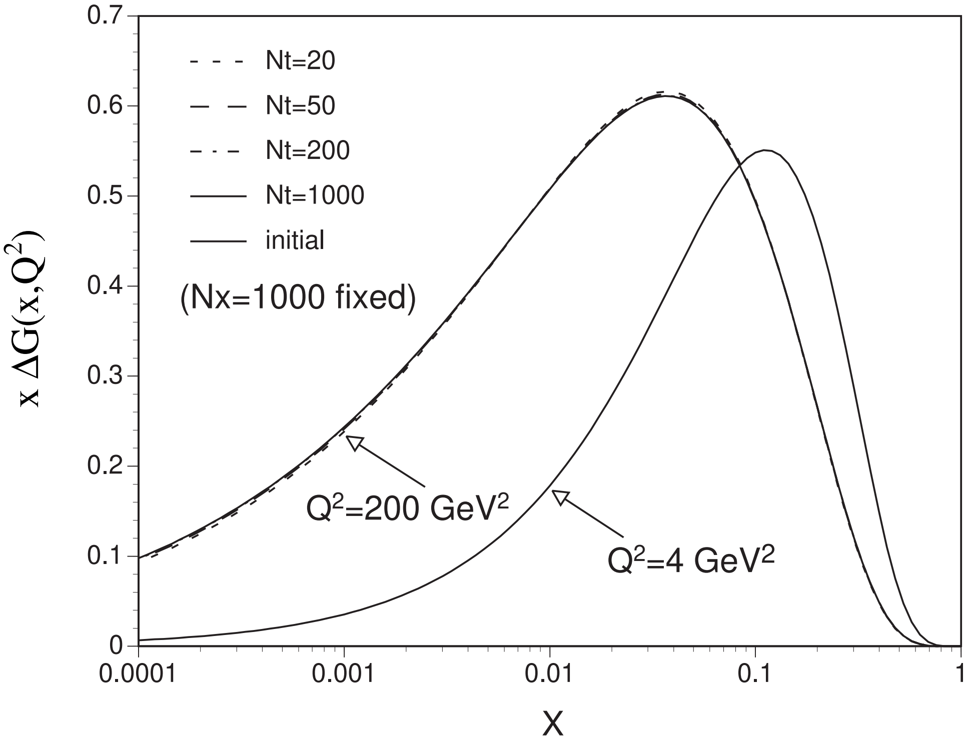

Figure 3: N_t dependence of gluon evolution results is shown. Notations are the same with those in Fig. 1.

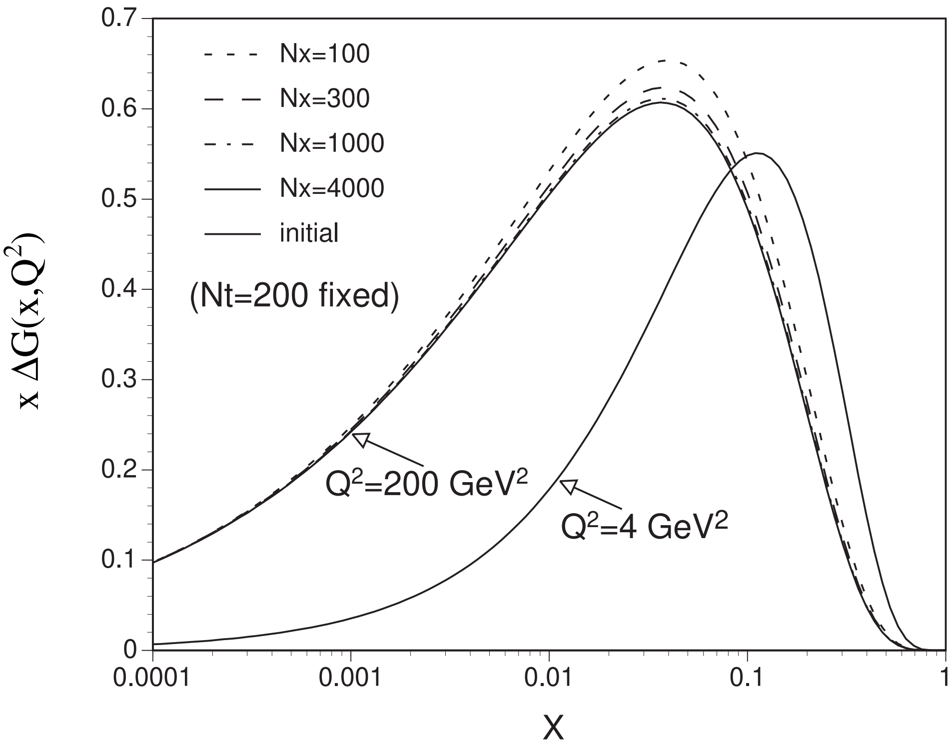

Figure 4: N_x dependence of gluon evolution results is shown. Notations are the same with those in Fig. 2.

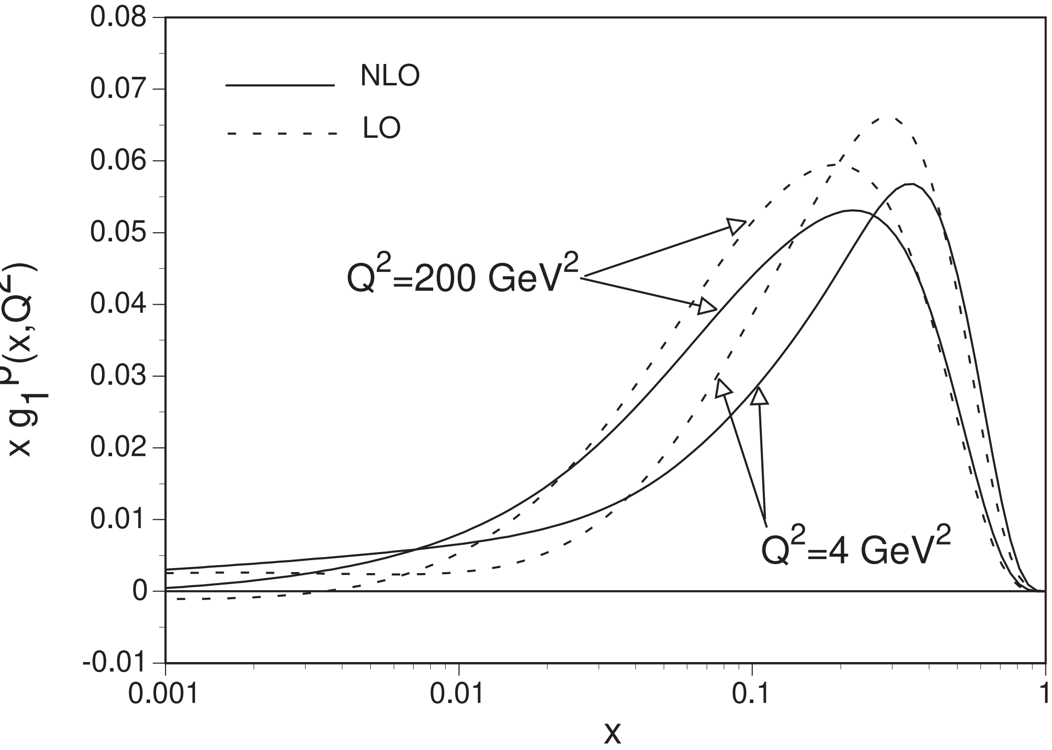

Figure 5: Q^2 evolution results for the proton structure function g_1 are shown. The solid curves are xg_1 at Q^2=4 and 200 GeV^2 in the NLO case, and the dashed ones are in the LO.

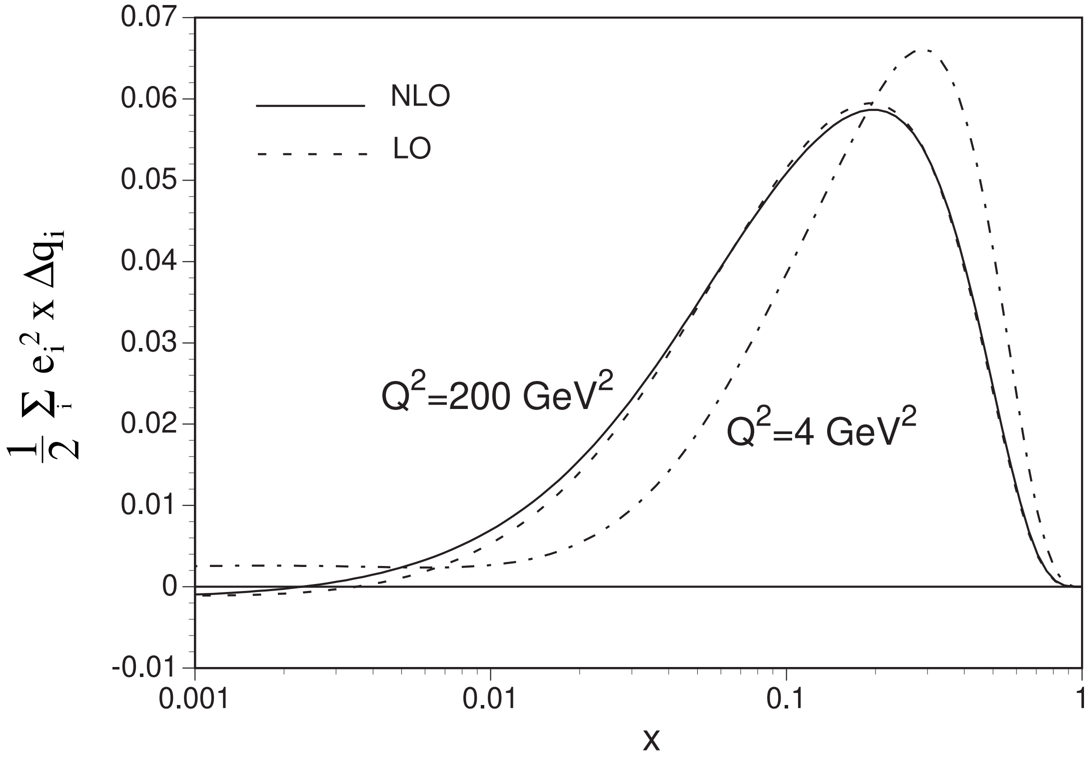

Figure 6: Q^2 evolution results for the distribution $\sum_i e_i^2\, x\, \Delta q_i/2$ are shown. The same distributions are assumed at Q^2=4 GeV^2 and the evolved distributions are shown by the solid curve in the NLO case and by the dashed one in the LO at 200 GeV^2.

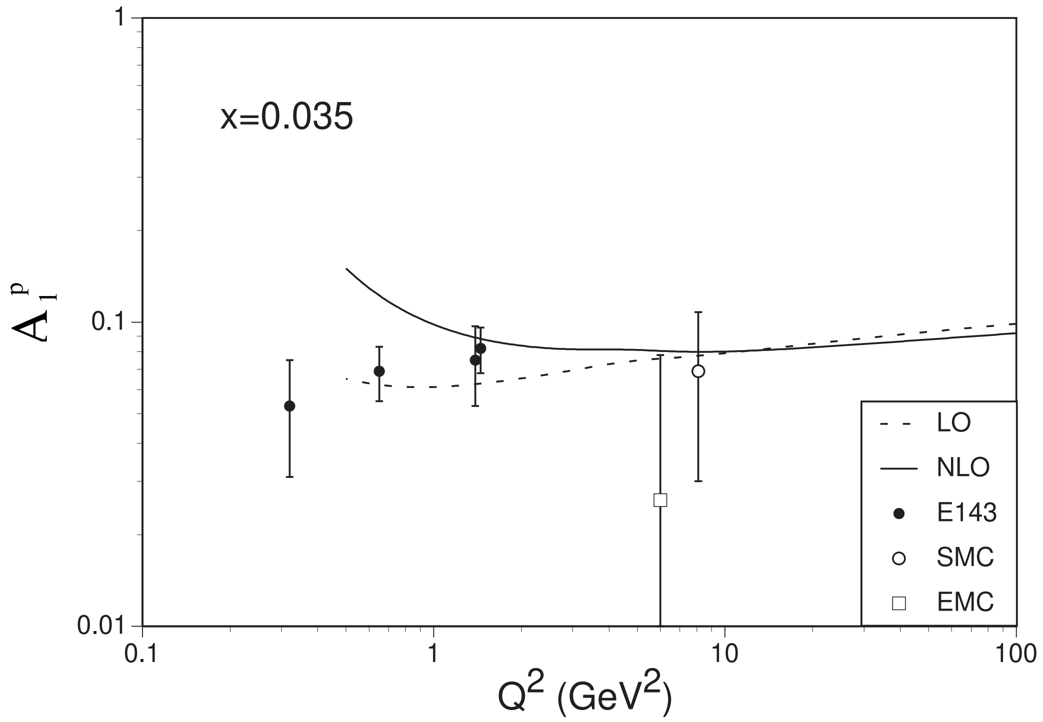

Figure 7: Q^2 dependence of the spin asymmetry A_1 for the proton is calculated in the LO and NLO cases. Calculated results at $x = 0.035$ are compared with SLAC-143 [13], EMC [14], and SMC [15] experimental data. The solid curve is in the NLO case and the dashed one is in the LO.

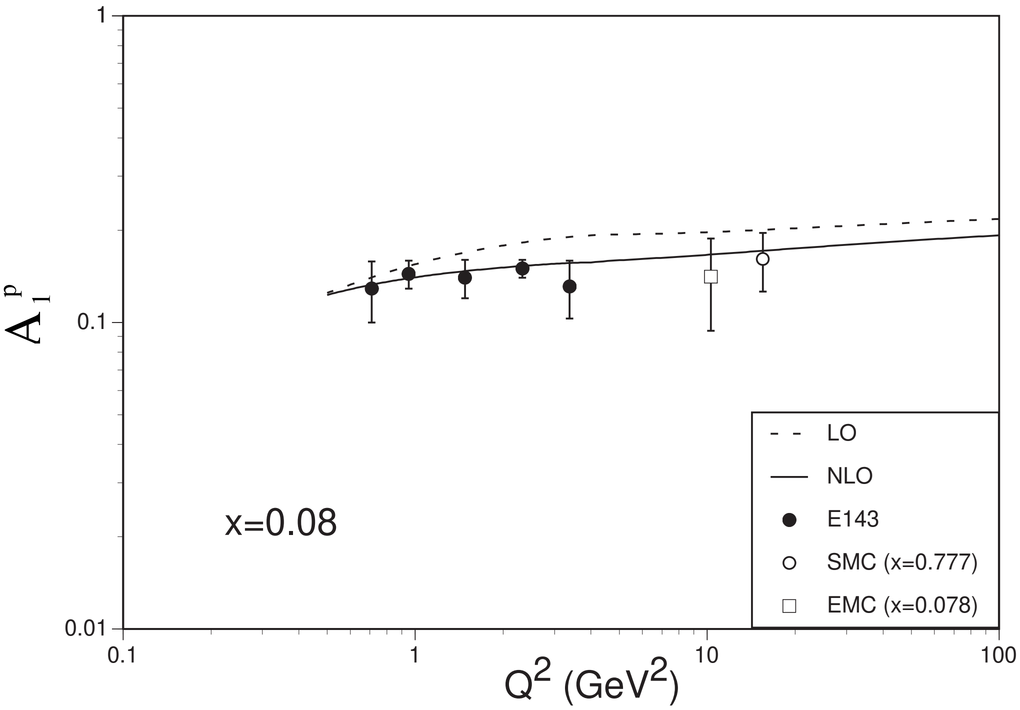

Figure 8: Q^2 dependence of the spin asymmetry A_1 at $x = 0.08$. Notations are same with those in Fig. 7.

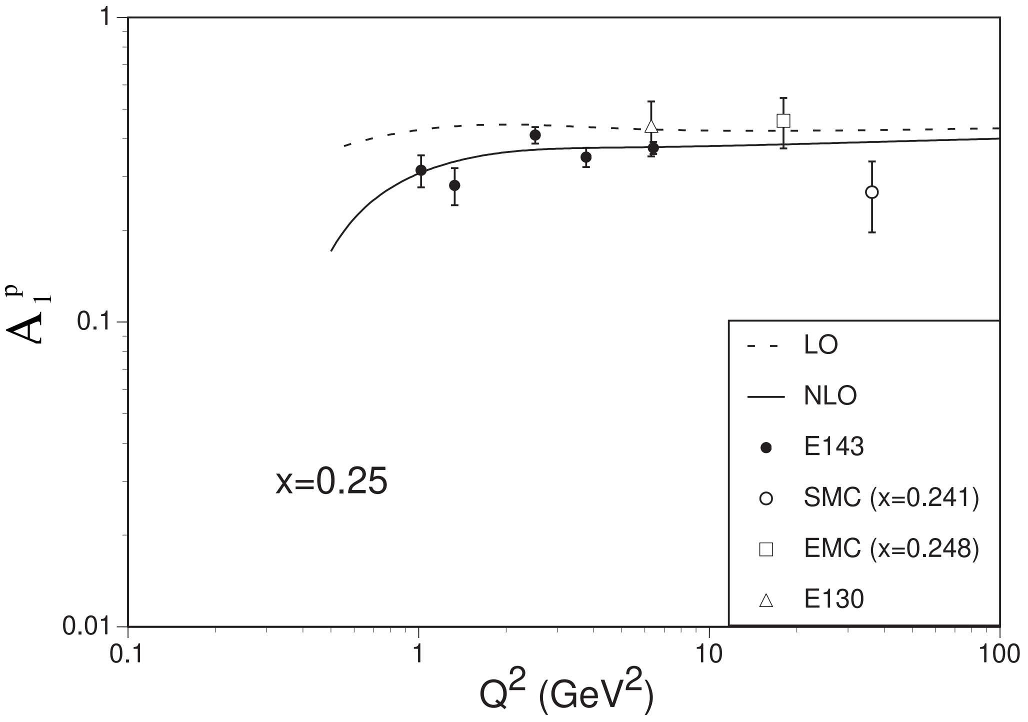

Figure 9: Q^2 dependence of the spin asymmetry A_1 at $x = 0.25$. Notations are same with those in Fig. 7. The SLAC-E130 data [12] is added.